

Single-phonon helium-atom scattering from Au(111)

M. Cates and D. R. Miller

Department of Applied Mechanics and Engineering Sciences, University of California, San Diego, California 92093

(Received 28 March 1983; revised manuscript received 7 June 1983)

We recently reported on preliminary surface-phonon-dispersion data for Au(111) obtained by helium atom scattering [M. Cates and D. R. Miller, *J. Electron Spectrosc. Relat. Phenom.* **30**, 157 (1982)]. We report in this paper additional scattering data, inelastic scattering probabilities, and a comparison of our spectra to theoretical calculations.

The use of low-energy helium atom scattering as a probe of surface phonons has been well substantiated for LiF.¹ For metals the published results have been preliminary²⁻⁴; results on Ag(111) with excellent resolution have recently been obtained.⁵ We have chosen to work with a very smooth metal surface to reduce the complexity of the scattering problem due to resonant coupling of the phonon processes to diffraction channels. It may then be possible that a perturbative calculation would be applicable and that the effect of the conduction electrons on the effective interaction potential for the single-phonon scattering of helium atoms can be assessed.

Our apparatus and procedures have been described previously.⁶ For these experiments a cooled helium source was used to provide a beam resolution of 3% [full width at half maximum (FWHM)] and a mean energy of 22 meV. The crystal was oriented with low-energy electron diffraction (LEED) and the cleanliness verified with Auger. We have not been able to observe helium or hydrogen diffraction reproducibly, and we have put an upper limit on the diffraction probabilities of 10^{-5} . Integration of the scattering under the specular peak, 1.2° FWHM, accounts for 40–80% of the incident beam intensity depending upon whether one assumes out-of-plane symmetry about the specular peak. Since most of the incident beam intensity is accounted for in these systems it seems possible that quantitative values for the differential scattering cross sections can be obtained.

Figures 1 and 2 show two examples of our raw time-of-flight data, while Fig. 3 shows the dispersion curves for the bottom of the bulk bands and for the Rayleigh surface mode, along the $\langle 11\bar{2} \rangle$ direction. The two theoretical curves represent lattice calculations by Black⁷ and Nizzoli.⁸ The data, from several runs, were obtained by fitting the leading edge of the inelastic time-of-flight peak. The scatter in these data is one measure of our uncertainty in determining the leading-edge position (as well as our reproducibility). Another is indicated by the error bar shown in Fig. 3 near the zone edge. This error bar indicates the best timing accuracy, 1 μ sec, of which our electronics is capable. In Figs. 1 and 2 we have shown the numerical time-of-flight curve generated from the theoretical Rayleigh phonon dispersion curves shown in Fig. 3. These numerical fits were generated with use of the measured incident-beam velocity and angle distributions, scattering from the Rayleigh phonons of the crystal with a probability given by the solid line in Fig. 4, and passage into the detector with kinematic constraints determined by the usual single-phonon, in-plane conservation equations, using only the first zone about specular.

The incoherent elastic background peaks (the smaller peaks at longer times) were fitted with the measured elastic time-of-flight spectrum and can be easily subtracted from the inelastic spectrum. Figure 2 is representative of our worst signal-to-noise data. Figure 1 is a compromise between our best signal-to-noise ratio and good separation from the elastic background.

We have placed indications on Fig. 3 for the Rayleigh phonons which would be responsible for the data in Figs. 1 and 2. In Fig. 1, the scattering intensity at smaller arrival times (due to higher-frequency phonon annihilation) not modeled by Rayleigh scattering is a clear indication that there is significant contribution to the scattering at this ω, Q because of bulk phonons. The bulk-phonon contribution to the data nearer the zone edge (Fig. 2) is reduced because the gap between the Rayleigh phonons and the bottom edge of the bulk modes is larger near the zone edge, and, irrespective of polarization, we expect the cross section to diminish rapidly with ω , as shown in Fig. 4. Rayleigh phonons are expected to contribute significantly to the scattering under our conditions because they have the desirable e_z polarization and they contribute significantly to the total displacement amplitude at the surface. Calculations by Nizzoli have indicated that the Rayleigh contribution to the peak intensity of our data varies from about 40% to 80% as we

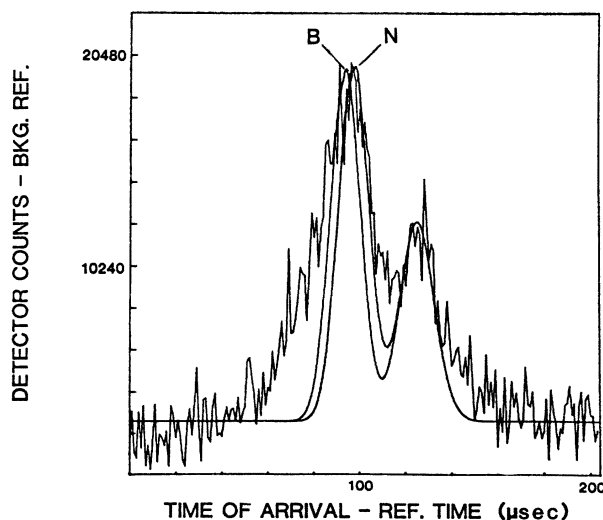


FIG. 1. Time-of-flight data for He on Au(111) in the $\langle 11\bar{2} \rangle$ direction. $\theta_i = 65.0^\circ$, $\theta_s = 50.0^\circ$, $E_i = 21.9$ meV, $T_s = 140$ K. The solid lines are numerical results using the dispersion curves of Black and Nizzoli. The incoherent elastic peaks are to the right.

move toward the zone edge.

Because the bulk-phonon contribution is not well separated from the Rayleigh phonon scattering, the best measure of the Rayleigh phonon dispersion curve is the leading edge of the time-of-flight spectrum (the edge nearest the elastic peak). As indicated in Figs. 1 and 2 the dispersion curve of Nizzoli provides the best prediction of this critical part of the time-of-flight spectrum. This was generally true in all of our fits and we would therefore suggest that the Nizzoli curve shown in Fig. 3 is the better Rayleigh dispersion curve for the Au(111) surface.

Figure 4 shows the experimental, inelastic scattering probabilities we have obtained by convolution with the Rayleigh phonon curve from six independent sets of runs, each normalized by the specular peak. The solid line is a mean of these data, indicating a rapid falloff of cross section near the zone edge. The average value of the ratio of the specular intensity to the incident beam intensity is 0.20. Since, as we noted above, bulk phonons could also contribute, these probabilities may be high.

Finally, in Fig. 4 we have shown as a dashed curve the computed relative scattering probability based on the single-phonon calculation of Cabrera, Celli, Goodman, and Manson²:

$$\frac{\partial^2 P^{(1)}}{\partial E_f \partial \Omega_f} = \frac{\mu \nu_a M_B k_f}{4\pi^2 \hbar^3 L_z k_{sz}} \sum_{\nu} \frac{e_{mz}^2}{\omega_m} |(E_f \cos^2 \theta_f | L_z \nu | E_i \cos^2 \theta_i)| \left[\left(\frac{\delta(E_f - E_i + \hbar \omega_m)}{1 - \exp(-\hbar \omega_m / k_B T_s)} \right) \bar{Q} - \bar{K}_i - \bar{K}_f \right] + \left(\frac{\delta(E_i - E_f + \hbar \omega_m)}{\exp(\hbar \omega_m / k_B T_s) - 1} \right) \bar{Q} - \bar{K}_f - \bar{K}_i \right],$$

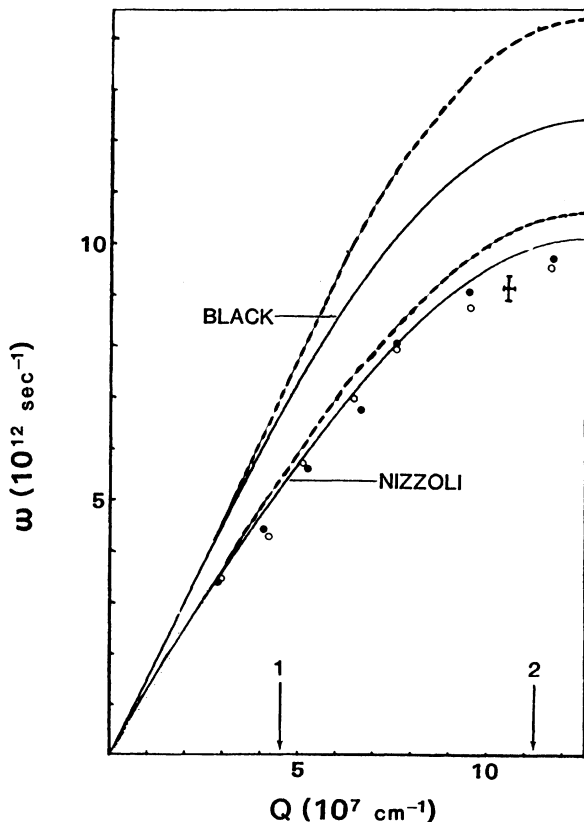


FIG. 3. Dispersion curves for He on Au(111). Solid curves are the Rayleigh modes, dashed are the bottom of the bulk bands. The experimental data are obtained by fitting the leading edge of the time-of-flight curves. Arrows show conditions of Figs. 1 and 2.

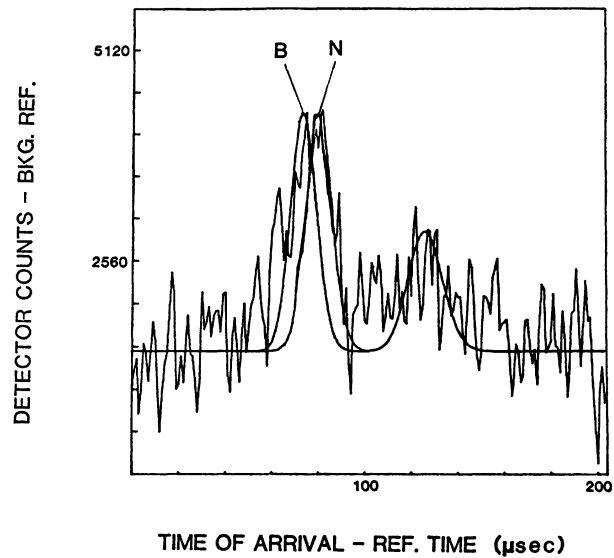


FIG. 2. Time-of-flight data for He on Au(111) in the $\langle 11\bar{2} \rangle$ direction. $\theta_1 = 65.0^\circ$, $\theta_2 = 39.7^\circ$, $E_i = 21.8$ meV, $T_s = 140$ K. Incoherent elastic peaks to the right.

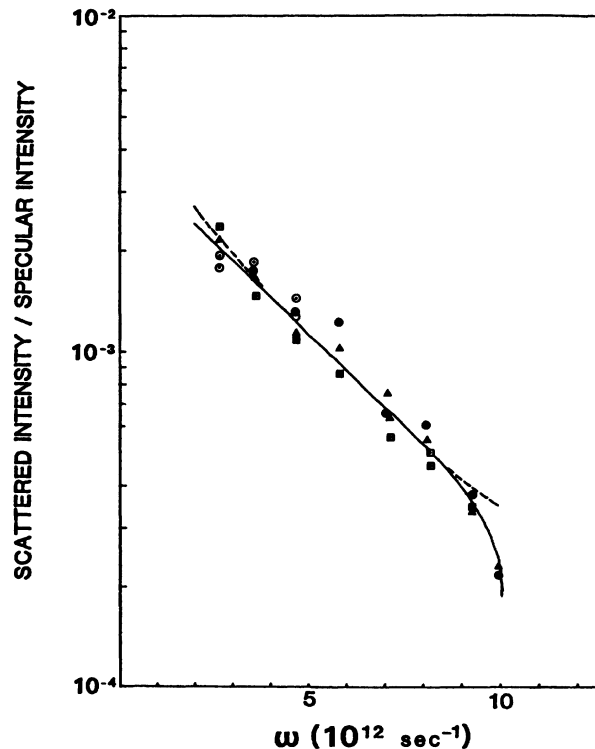


FIG. 4. Deconvoluted peak intensities of single-phonon annihilation, assuming Rayleigh phonons, normalized by specular intensity. Dotted line is the theoretical curve; solid line is the mean of the data points.

where the nomenclature is identical to that given in Ref. 9. For a soft exponential repulsion of the type $V = e^{-2az}$ the matrix element is⁹

$$-(E_f \cos^2 \theta_f | L_z \nu_0 | E_i \cos^2 \theta_i) = \frac{\hbar^2 a^2 \pi}{M_g} [\beta_f \beta_i \sinh(\pi \beta_f) \sinh(\pi \beta_i)]^{1/2} \frac{\beta_f^2 - \beta_i^2}{\cosh(\pi \beta_f) - \cosh(\pi \beta_i)}.$$

We have taken $e_{mz}^2 = Q/G$,¹⁰ and the softness parameter a to be $1.75A^{-1}$. The cross section was calculated for Rayleigh phonon annihilation only, with use of Nizzoli's dispersion curve, with surface temperature = 140 K, incident energy = 22.0 meV, and incident angle = 65°. The curve was fitted to the data at $\omega = 5.0 \times 10^{12} \text{ sec}^{-1}$ to assess the relative ω dependence.

As Fig. 4 shows, this cross section fits the data very well except near the zone edge, where the experimental probability decreases rapidly. This may be due to the softness of the repulsive potential or to the conduction electrons smoothing the lateral potential (reducing the corrugation) for large displacements near the zone edge. Additionally, for a quantitative comparison, future analysis should include not only the bulk modes, but the Debye-Waller factor as

well as the Beeby correction for the attractive well.

Although additional data with better resolution are desirable to clearly separate the bulk-phonon contribution, especially at low ω , we feel these data are consistent with a significant Rayleigh phonon interaction. Under the assumption that this is true, the data then determine the position of the Rayleigh phonon dispersion curve to within the accuracy indicated by Fig. 3 and, to within factors of 2, give the correct scattering probabilities.

ACKNOWLEDGMENT

This research was supported by the National Science Foundation under Grant No. DMR-8108425.

¹G. Brusdeylins, R. Doak, and J. Toennies, Phys. Rev. Lett. **44**, 1417 (1980); **46**, 437 (1980).

²S. Yerkes and D. R. Miller, J. Vac. Sci. Technol. **17**, 126 (1980).

³B. F. Mason and B. R. Williams, Phys. Rev. Lett. **46**, 1138 (1981).

⁴B. Feuerbacher and R. F. Willis, Phys. Rev. Lett. **47**, 526 (1981).

⁵R. Doak, U. Harten, and J. P. Toennies (private communication).

⁶J. Horne, S. Yerkes, and D. R. Miller, Surf. Sci. **93**, 47 (1980).

⁷J. E. Black, Brock University, Canada (private communication).

⁸F. Nizzoli, Università di Modena, Italy (private communication).

⁹F. O. Goodman and H. Y. Wachman, *Dynamics of Gas-Surface Scattering* (Academic, New York, 1976), pp. 175 and 180.

¹⁰Hans-Dieter Meyer, Surf. Sci. **104**, 117 (1981).